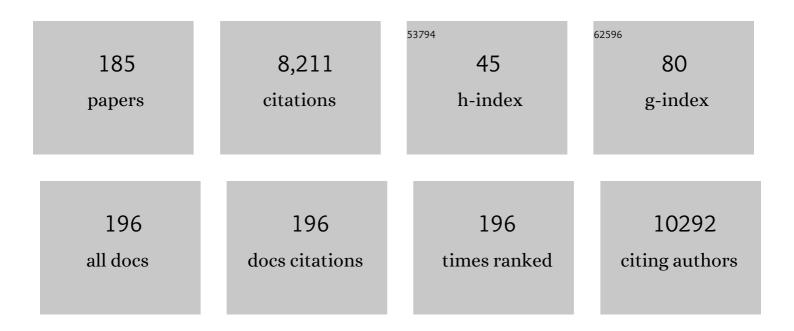
Danny J J Wang

List of Publications by Year in descending order

Source: https://exaly.com/author-pdf/2797314/publications.pdf Version: 2024-02-01



DANNY LL MANC

#	Article	IF	CITATIONS
1	Massively parallel functional photoacoustic computed tomography of the human brain. Nature Biomedical Engineering, 2022, 6, 584-592.	22.5	97
2	Optimization of pseudoâ€continuous arterial spin labeling at 7T with parallel transmission B1 shimming. Magnetic Resonance in Medicine, 2022, 87, 249-262.	3.0	10
3	k-space weighted image average (KWIA) for ASL-based dynamic MR angiography and perfusion imaging. Magnetic Resonance Imaging, 2022, 86, 94-106.	1.8	0
4	Editorial for "Multiâ€planar, multiâ€contrast and multiâ€time point analysis tool (<scp>MOCHA</scp>) for intracranial vessel wall characterization― Journal of Magnetic Resonance Imaging, 2022, 56, 956-957.	3.4	0
5	Selective vulnerability of medial temporal regions to short-term blood pressure variability and cerebral hypoperfusion in older adults. NeuroImage Reports, 2022, 2, 100080.	1.0	7
6	Modulation of brain networks during MR-compatible transcranial direct current stimulation. NeuroImage, 2022, 250, 118874.	4.2	11
7	Instrumental validation of free water, peakâ€width of skeletonized mean diffusivity, and white matter hyperintensities: MarkVCID neuroimaging kits. Alzheimer's and Dementia: Diagnosis, Assessment and Disease Monitoring, 2022, 14, e12261.	2.4	25
8	Effects of Repetitive Peripheral Sensory Stimulation in the Subacute and Chronic Phases After Stroke: Study Protocol for a Pilot Randomized Trial. Frontiers in Neurology, 2022, 13, 779128.	2.4	0
9	Association of Intensive vs Standard Blood Pressure Control With Cerebral Blood Flow. JAMA Neurology, 2022, 79, 380.	9.0	26
10	Cerebrovascular reactivity deficits in cognitively unimpaired older adults: vasodilatory versus vasoconstrictive responses. Neurobiology of Aging, 2022, 113, 55-62.	3.1	8
11	Pathophysiological Mechanisms Underlying Idiopathic Normal Pressure Hydrocephalus: A Review of Recent Insights. Frontiers in Aging Neuroscience, 2022, 14, 866313.	3.4	9
12	Cerebroarterial pulsatility and resistivity indices are associated with cognitive impairment and white matter hyperintensity in elderly subjects: A phase-contrast MRI study. Journal of Cerebral Blood Flow and Metabolism, 2021, 41, 670-683.	4.3	14
13	Cerebral perfusion is associated with blast exposure in military personnel without moderate or severe TBI. Journal of Cerebral Blood Flow and Metabolism, 2021, 41, 886-900.	4.3	14
14	High-Resolution Neurovascular Imaging at 7T. Magnetic Resonance Imaging Clinics of North America, 2021, 29, 53-65.	1.1	9
15	Brain arteriolosclerosis. Acta Neuropathologica, 2021, 141, 1-24.	7.7	85
16	Optimization of adiabatic pulses for pulsed arterial spin labeling at 7 tesla: Comparison with pseudo ontinuous arterial spin labeling. Magnetic Resonance in Medicine, 2021, 85, 3227-3240.	3.0	11
17	In-vivo imaging of targeting and modulation of depression-relevant circuitry by transcranial direct current stimulation: a randomized clinical trial. Translational Psychiatry, 2021, 11, 138.	4.8	12
18	Assessment of carotid stiffness by measuring carotid pulse wave velocity using a singleâ€slice obliqueâ€sagittal phaseâ€contrast MRI. Magnetic Resonance in Medicine, 2021, 86, 442-455.	3.0	5

#	Article	IF	CITATIONS
19	Retrospective motion artifact correction of structural MRI images using deep learning improves the quality of cortical surface reconstructions. NeuroImage, 2021, 230, 117756.	4.2	39
20	Water exchange rate across the bloodâ€brain barrier is associated with CSF amyloidâ€Î² 42 in healthy older adults. Alzheimer's and Dementia, 2021, 17, 2020-2029.	0.8	31
21	A novel technique for accurate electrode placement over cortical targets for transcranial electrical stimulation (tES) clinical trials. Journal of Neural Engineering, 2021, 18, .	3.5	5
22	Evaluation of Cerebral Blood Flow Measured by 3D PCASL as Biomarker of Vascular Cognitive Impairment and Dementia (VCID) in a Cohort of Elderly Latinx Subjects at Risk of Small Vessel Disease. Frontiers in Neuroscience, 2021, 15, 627627.	2.8	25
23	MarkVCID cerebral small vessel consortium: II. Neuroimaging protocols. Alzheimer's and Dementia, 2021, 17, 716-725.	0.8	45
24	Super-Resolution Arterial Spin Labeling Using Slice-Dithered Enhanced Resolution and Simultaneous Multi-Slice Acquisition. Frontiers in Neuroscience, 2021, 15, 737525.	2.8	5
25	Noncontrast Pediatric Brain Perfusion. Magnetic Resonance Imaging Clinics of North America, 2021, 29, 493-513.	1.1	4
26	Cerebral perfusion and neurological examination characterise neonatal opioid withdrawal syndrome: a prospective cohort study. Archives of Disease in Childhood: Fetal and Neonatal Edition, 2021, , fetalneonatal-2021-322192.	2.8	2
27	Semiautomatic cerebrovascular territory mapping based on dynamic ASL MR angiography without vesselâ€encoded labeling. Magnetic Resonance in Medicine, 2021, 85, 2735-2746.	3.0	2
28	Advanced pCASL pediatric perfusion MRI. Advances in Magnetic Resonance Technology and Applications, 2021, , 89-111.	0.1	0
29	Multi-vendor and multisite evaluation of cerebrovascular reactivity mapping using hypercapnia challenge. NeuroImage, 2021, 245, 118754.	4.2	7
30	Laminar perfusion imaging with zoomed arterial spin labeling at 7 Tesla. Neurolmage, 2021, 245, 118724.	4.2	11
31	Dynamics of the cerebral blood flow response to brief neural activity in human visual cortex. Journal of Cerebral Blood Flow and Metabolism, 2020, 40, 1823-1837.	4.3	13
32	Associations between cerebral blood flow and structural and functional brain imaging measures in individuals with neuropsychologically defined mild cognitive impairment. Neurobiology of Aging, 2020, 86, 64-74.	3.1	42
33	Robust single-shot acquisition of high resolution whole brain ASL images by combining time-dependent 2D CAPIRINHA sampling with spatio-temporal TGV reconstruction. NeuroImage, 2020, 206, 116337.	4.2	26
34	Human Placenta Blood Flow During Early Gestation With Pseudocontinuous Arterial Spin Labeling MRI. Journal of Magnetic Resonance Imaging, 2020, 51, 1247-1257.	3.4	23
35	Consensus-based technical recommendations for clinical translation of renal ASL MRI. Magnetic Resonance Materials in Physics, Biology, and Medicine, 2020, 33, 141-161.	2.0	80
36	Deep Learning Detection of Penumbral Tissue on Arterial Spin Labeling in Stroke. Stroke, 2020, 51, 489-497.	2.0	39

#	Article	IF	CITATIONS
37	Genetic Control Over Cerebral Blood Flow and Resting State Regional Homogeneity Signal. Biological Psychiatry, 2020, 87, S397-S398.	1.3	Ο
38	Layer-dependent multiplicative effects of spatial attention on contrast responses in human early visual cortex. Progress in Neurobiology, 2020, 207, 101897.	5.7	15
39	Lower retinal capillary density in minimal cognitive impairment among older Latinx adults. Alzheimer's and Dementia: Diagnosis, Assessment and Disease Monitoring, 2020, 12, e12071.	2.4	10
40	Comparison Between Blood-Brain Barrier Water Exchange Rate and Permeability to Gadolinium-Based Contrast Agent in an Elderly Cohort. Frontiers in Neuroscience, 2020, 14, 571480.	2.8	30
41	Water exchange across bloodâ€brain barrier is associated with CSF amyloidâ€42 level in healthy older adults. Alzheimer's and Dementia, 2020, 16, e036794.	0.8	1
42	Bloodâ€brain barrier dysfunction and perioperative neurocognitive disorders: Cognitive Recovery after Elective Surgery (CREATES) study design and methods. Alzheimer's and Dementia, 2020, 16, e039363.	0.8	0
43	Mean arterial pressure during cerebral perfusion MRI: An arterial spinâ€labeling study in younger and older adults. Alzheimer's and Dementia, 2020, 16, e043623.	0.8	Ο
44	fMRI complexity is associated with tauâ€PET and cognitive decline in Alzheimer's disease. Alzheimer's and Dementia, 2020, 16, e045411.	0.8	1
45	Detection of attenuated dynamic cerebrovascular function in aging and cognitive decline using a novel neuroimaging approach. Alzheimer's and Dementia, 2020, 16, e045968.	0.8	Ο
46	Plasma tau is negatively correlated with frontal lobe CBF in hypertensive adults on the AD spectrum. Alzheimer's and Dementia, 2020, 16, e046355.	0.8	0
47	Concurrent Imaging of Markers of Current Flow and Neurophysiological Changes During tDCS. Frontiers in Neuroscience, 2020, 14, 374.	2.8	11
48	Reperfusion Into Severely Damaged Brain Tissue Is Associated With Occurrence of Parenchymal Hemorrhage for Acute Ischemic Stroke. Frontiers in Neurology, 2020, 11, 586.	2.4	7
49	Low Dose CT Perfusion With K-Space Weighted Image Average (KWIA). IEEE Transactions on Medical Imaging, 2020, 39, 3879-3890.	8.9	5
50	Single and repeated ketamine treatment induces perfusion changes in sensory and limbic networks in major depressive disorder. European Neuropsychopharmacology, 2020, 33, 89-100.	0.7	27
51	Editorial: Advances in Multi-Scale Analysis of Brain Complexity. Frontiers in Neuroscience, 2020, 14, 337.	2.8	3
52	Robust functional mapping of layer-selective responses in human lateral geniculate nucleus with high-resolution 7T fMRI. Proceedings of the Royal Society B: Biological Sciences, 2020, 287, 20200245.	2.6	14
53	Abstract 13327: Worse Cerebral Blood Flow in Single Right verses Left Ventricle After Fontan Completion. Circulation, 2020, 142, .	1.6	0
54	An Automatic Estimation of Arterial Input Function Based on Multi-Stream 3D CNN. Frontiers in Neuroinformatics, 2019, 13, 49.	2.5	18

#	Article	IF	CITATIONS
55	Characterization of lenticulostriate arteries with high resolution black-blood T1-weighted turbo spin echo with variable flip angles at 3 and 7†Tesla. NeuroImage, 2019, 199, 184-193.	4.2	24
56	A review of transcranial direct current stimulation (tDCS) for the individualized treatment of depressive symptoms. Personalized Medicine in Psychiatry, 2019, 17-18, 17-22.	0.1	19
57	Quantification of intracranial arterial blood flow using noncontrast enhanced 4D dynamic MR angiography. Magnetic Resonance in Medicine, 2019, 82, 449-459.	3.0	10
58	Recent Advances in Pediatric Brain, Spine, and Neuromuscular Magnetic Resonance Imaging Techniques. Pediatric Neurology, 2019, 96, 7-23.	2.1	8
59	ICâ€Pâ€085: CHARACTERIZATION OF LENTICULOSTRIATE ARTERIES USING ARTERIAL SPIN LABELING AND HIGHâ€RESOLUTION 3D BLACKâ€BLOOD MRI AS AN IMAGING MARKER IN VASCULAR COGNITIVE IMPAIRMENT AI DEMENTIA. Alzheimer's and Dementia, 2019, 15, P75.	N D .8	0
60	ICâ€Pâ€041: STRATEGIES OF BRAIN MRI DATA ACQUISITION, QUALITY CONTROL AND ANALYSIS FOR THE MULTICENTER RISK REDUCTION FOR ALZHEIMER'S DISEASE (RRAD) CLINICAL TRIAL. Alzheimer's and Dementia, 2019, 15, P45.	0.8	0
61	Differences in high-definition transcranial direct current stimulation over the motor hotspot versus the premotor cortex on motor network excitability. Scientific Reports, 2019, 9, 17605.	3.3	22
62	Hypercapnia increases brain viscoelasticity. Journal of Cerebral Blood Flow and Metabolism, 2019, 39, 2445-2455.	4.3	28
63	Mapping water exchange across the blood–brain barrier using 3D diffusionâ€prepared arterial spin labeled perfusion MRI. Magnetic Resonance in Medicine, 2019, 81, 3065-3079.	3.0	80
64	Multi-phase 3D arterial spin labeling brain MRI in assessing cerebral blood perfusion and arterial transit times in children at 3T. Clinical Imaging, 2019, 53, 210-220.	1.5	15
65	Vascular dysfunction—The disregarded partner of Alzheimer's disease. Alzheimer's and Dementia, 2019, 15, 158-167.	0.8	454
66	Clinical 7 T MRI: Are we there yet? A review about magnetic resonance imaging at ultra-high field. British Journal of Radiology, 2019, 92, 20180492.	2.2	66
67	Multidelay multiparametric arterial spin labeling perfusion MRI and mild cognitive impairment in early stage Parkinson's disease. Human Brain Mapping, 2019, 40, 1317-1327.	3.6	28
68	7-Tesla MRI of the brain in a research subject with bilateral, total knee replacement implants: Case report and proposed safety guidelines. Magnetic Resonance Imaging, 2019, 57, 313-316.	1.8	5
69	Collateral perfusion using arterial spin labeling in symptomatic versus asymptomatic middle cerebral artery stenosis. Journal of Cerebral Blood Flow and Metabolism, 2019, 39, 108-117.	4.3	31
70	Value of pituitary gland MRI at 7 T in Cushing's disease and relationship to inferior petrosal sinus sampling: case report. Journal of Neurosurgery, 2019, 130, 347-351.	1.6	13
71	Regional association of pCASL-MRI with FDG-PET and PiB-PET in people at risk for autosomal dominant Alzheimer's disease. NeuroImage: Clinical, 2018, 17, 751-760.	2.7	27
72	ASPECTS-based reperfusion status on arterial spin labeling is associated with clinical outcome in acute ischemic stroke patients. Journal of Cerebral Blood Flow and Metabolism, 2018, 38, 382-392.	4.3	24

#	Article	IF	CITATIONS
73	A constrained sliceâ€dependent background suppression scheme for simultaneous multislice pseudoâ€continuous arterial spin labeling. Magnetic Resonance in Medicine, 2018, 79, 394-400.	3.0	28
74	Accelerated noncontrastâ€enhanced 4â€dimensional intracranial MR angiography using goldenâ€angle stackâ€ofâ€stars trajectory and compressed sensing with magnitude subtraction. Magnetic Resonance in Medicine, 2018, 79, 867-878.	3.0	28
75	Lowâ€dose <scp>CT</scp> perfusion with projection view sharing. Medical Physics, 2018, 45, 101-113.	3.0	5
76	Noncontrastâ€enhanced timeâ€resolved 4D dynamic intracranial MR angiography at 7T: A feasibility study. Journal of Magnetic Resonance Imaging, 2018, 48, 111-120.	3.4	16
77	Measuring human placental blood flow with multidelay 3D GRASE pseudocontinuous arterial spin labeling at 3T. Journal of Magnetic Resonance Imaging, 2018, 47, 1667-1676.	3.4	37
78	DTâ€02â€05: MARKVCID PHASE II: PRIORITIZED CANDIDATE SMALL VESSEL VCID BIOMARKERS SELECTED FOR INDEPENDENT MULTI‧ITE TESTING AND VALIDATION. Alzheimer's and Dementia, 2018, 14, P1670.	0.8	3
79	P2â€100: IMPACT OF HYPERTENSION ON INTRACRANIAL ARTERIAL COMPLIANCE IN A LATINO COHORT. Alzheimer's and Dementia, 2018, 14, P706.	0.8	0
80	P2â€369: MEASURING WATER EXCHANGE ACROSS BLOOD BRAIN BARRIER IN ELDERLY SUBJECTS BY DIFFUSION WEIGHTED PSEUDOâ€CONTINUOUS ARTERIAL SPIN LABELING. Alzheimer's and Dementia, 2018, 14, P835.	0.8	1
81	ICâ€Pâ€059: REVEALING SMALL SUBFIELDS OF HIPPOCAMPUS IN VIVO WITH 7T STRUCTURAL MRI. Alzheimer's a Dementia, 2018, 14, P55.	nd 0.8	5
82	O5â€01â€06: HIGH RESOLUTION 3D BLACK BLOOD MRI OF HUMAN LENTICULOSTRIATE ARTERIES AS AN IMAGIN BIOMARKER FOR VASCULAR COGNITIVE IMPAIRMENT AND DEMENTIA. Alzheimer's and Dementia, 2018, 14, P1641.	VG 0.8	0
83	Imbalance of Functional Connectivity and Temporal Entropy in Resting-State Networks in Autism Spectrum Disorder: A Machine Learning Approach. Frontiers in Neuroscience, 2018, 12, 869.	2.8	12
84	Default Mode Network Complexity and Cognitive Decline in Mild Alzheimer's Disease. Frontiers in Neuroscience, 2018, 12, 770.	2.8	103
85	Neurophysiological Basis of Multi-Scale Entropy of Brain Complexity and Its Relationship With Functional Connectivity. Frontiers in Neuroscience, 2018, 12, 352.	2.8	90
86	Improved sensitivity of cellular MRI using phase-cycled balanced SSFP of ferumoxytol nanocomplex-labeled macrophages at ultrahigh field. International Journal of Nanomedicine, 2018, Volume 13, 3839-3852.	6.7	3
87	Abstract WP60: Kernel Spectral Regression and Neural Networks Enable Regional Detection of Hemorrhagic Transformation on Multi-Modal MRI for Acute Ischemic Stroke. Stroke, 2018, 49, .	2.0	1
88	Abstract WP419: Visualization and Evaluation of Human Lenticulostriate Arteries Using High-resolution Black-blood T1-weighted Turbo-spin Echo (TSE) at 3T and 7T. Stroke, 2018, 49, .	2.0	0
89	Abstract WMP24: Reperfusion Into Severely Damaged Brain Tissue is Associated With Impending Parenchymal Hemorrhage in Acute Ischemic Stroke Patients. Stroke, 2018, 49, .	2.0	0
90	A longitudinal study of cerebral blood flow under hypoxia at high altitude using 3D pseudo-continuous arterial spin labeling. Scientific Reports, 2017, 7, 43246.	3.3	12

#	Article	IF	CITATIONS
91	Goldenâ€ratio rotated stackâ€ofâ€stars acquisition for improved volumetric <scp>MRI</scp> . Magnetic Resonance in Medicine, 2017, 78, 2290-2298.	3.0	35
92	Reduced regional cerebral blood flow in patients with heart failure. European Journal of Heart Failure, 2017, 19, 1294-1302.	7.1	75
93	Arterial spin labeling MRI is able to detect early hemodynamic changes in diabetic nephropathy. Journal of Magnetic Resonance Imaging, 2017, 46, 1810-1817.	3.4	73
94	Integrated SSFP for functional brain mapping at 7 T with reduced susceptibility artifact. Journal of Magnetic Resonance, 2017, 276, 22-30.	2.1	5
95	Application of arterial spin labeling perfusion MRI to differentiate benign from malignant intracranial meningiomas. European Journal of Radiology, 2017, 97, 31-36.	2.6	42
96	Differential diagnosis of mitochondrial encephalopathy with lactic acidosis and stroke-like episodes (MELAS) and ischemic stroke using 3D pseudocontinuous arterial spin labeling. Journal of Magnetic Resonance Imaging, 2017, 45, 199-206.	3.4	28
97	Altered Glutamate and Regional Cerebral Blood Flow Levels in Schizophrenia: A 1H-MRS and pCASL study. Neuropsychopharmacology, 2017, 42, 562-571.	5.4	46
98	Multi-phase passband balanced SSFP fMRI with 50 ms sampling rate at 7 Tesla enables high precision in resolving 100 ms neuronal events. Magnetic Resonance Imaging, 2017, 35, 20-28.	1.8	4
99	Highly Accelerated SSFP Imaging with Controlled Aliasing in Parallel Imaging and integrated-SSFP (CAIPI-iSSFP). Investigative Magnetic Resonance Imaging, 2017, 21, 210.	0.4	2
100	Cerebral Hemodynamic and White Matter Changes of Type 2 Diabetes Revealed by Multi-TI Arterial Spin Labeling and Double Inversion Recovery Sequence. Frontiers in Neurology, 2017, 8, 717.	2.4	19
101	Changes in Cerebral Blood Flow during an Alteration in Glycemic State in a Large Non-human Primate (Papio hamadryas sp.). Frontiers in Neuroscience, 2017, 11, 49.	2.8	4
102	Multi-delay ASL can identify leptomeningeal collateral perfusion in endovascular therapy of ischemic stroke. Oncotarget, 2017, 8, 2437-2443.	1.8	44
103	Prospective motion correction for 3D GRASE pCASL with volumetric navigators. Proceedings of the International Society for Magnetic Resonance in Medicine Scientific Meeting and Exhibition., 2017, 25, 0680.	0.5	7
104	Noise Reduction in Arterial Spin Labeling Based Functional Connectivity Using Nuisance Variables. Frontiers in Neuroscience, 2016, 10, 371.	2.8	13
105	Quantification of liver perfusion using multidelay pseudocontinuous arterial spin labeling. Journal of Magnetic Resonance Imaging, 2016, 43, 1046-1054.	3.4	10
106	In-vivo Imaging of Magnetic Fields Induced by Transcranial Direct Current Stimulation (tDCS) in Human Brain using MRI. Scientific Reports, 2016, 6, 34385.	3.3	52
107	How the heart speaks to the brain: neural activity during cardiorespiratory interoceptive stimulation. Philosophical Transactions of the Royal Society B: Biological Sciences, 2016, 371, 20160017.	4.0	55
108	Developmental trajectories of cerebral blood flow and oxidative metabolism at baseline and during working memory tasks. NeuroImage, 2016, 134, 587-596.	4.2	12

#	Article	IF	CITATIONS
109	Comparison of non-invasive MRI measurements of cerebral blood flow in a large multisite cohort. Journal of Cerebral Blood Flow and Metabolism, 2016, 36, 1244-1256.	4.3	57
110	Patterns of postictal cerebral perfusion in idiopathic generalized epilepsy: a multi-delay multi-parametric arterial spin labelling perfusion MRI study. Scientific Reports, 2016, 6, 28867.	3.3	17
111	Phaseâ€cycled simultaneous multislice balanced SSFP imaging with CAIPIRINHA for efficient banding reduction. Magnetic Resonance in Medicine, 2016, 76, 1764-1774.	3.0	16
112	Reduced perfusion in normalâ€appearing white matter in mild to moderate hypertension as revealed by 3D pseudocontinuous arterial spin labeling. Journal of Magnetic Resonance Imaging, 2016, 43, 635-643.	3.4	26
113	Arterial Spin Labeling Magnetic Resonance Imaging Estimation of Antegrade and Collateral Flow in Unilateral Middle Cerebral Artery Stenosis. Stroke, 2016, 47, 428-433.	2.0	48
114	Assessing intracranial vascular compliance using dynamic arterial spin labeling. NeuroImage, 2016, 124, 433-441.	4.2	35
115	Altered resting perfusion and functional connectivity of default mode network in youth with autism spectrum disorder. Brain and Behavior, 2015, 5, e00358.	2.2	77
116	The pediatric template of brain perfusion. Scientific Data, 2015, 2, 150003.	5.3	53
117	Perfusion shift from white to gray matter may account for processing speed deficits in schizophrenia. Human Brain Mapping, 2015, 36, 3793-3804.	3.6	28
118	Waveletâ€based regularity analysis reveals recurrent spatiotemporal behavior in restingâ€state fMRI. Human Brain Mapping, 2015, 36, 3603-3620.	3.6	26
119	Water Exchange across the Bloodâ€Brain Barrier in Obstructive Sleep Apnea: An MRI Diffusionâ€Weighted Pseudo ontinuous Arterial Spin Labeling Study. Journal of Neuroimaging, 2015, 25, 900-905.	2.0	51
120	Detecting Static and Dynamic Differences between Eyes-Closed and Eyes-Open Resting States Using ASL and BOLD fMRI. PLoS ONE, 2015, 10, e0121757.	2.5	59
121	Detection of hyperperfusion on arterial spin labeling using deep learning. , 2015, 2015, 1322-1327.		5
122	Recommended implementation of arterial spinâ€labeled perfusion MRI for clinical applications: A consensus of the ISMRM perfusion study group and the European consortium for ASL in dementia. Magnetic Resonance in Medicine, 2015, 73, spcone.	3.0	19
123	Functional connectivity in BOLD and CBF data: Similarity and reliability of resting brain networks. NeuroImage, 2015, 106, 111-122.	4.2	102
124	Eigenanatomy: Sparse dimensionality reduction for multi-modal medical image analysis. Methods, 2015, 73, 43-53.	3.8	15
125	Recommended implementation of arterial spin″abeled perfusion MRI for clinical applications: A consensus of the ISMRM perfusion study group and the European consortium for ASL in dementia. Magnetic Resonance in Medicine, 2015, 73, 102-116.	3.0	1,663
126	Postischemic Hyperperfusion on Arterial Spin Labeled Perfusion MRI is Linked to Hemorrhagic Transformation in Stroke. Journal of Cerebral Blood Flow and Metabolism, 2015, 35, 630-637.	4.3	98

#	Article	IF	CITATIONS
127	Towards the identification of multi-parametric quantitative MRI biomarkers in lupus nephritis. Magnetic Resonance Imaging, 2015, 33, 1066-1074.	1.8	34
128	Reliability comparison of spontaneous brain activities between BOLD and CBF contrasts in eyes-open and eyes-closed resting states. NeuroImage, 2015, 121, 91-105.	4.2	66
129	Astrocytic tumour grading: a comparative study of three-dimensional pseudocontinuous arterial spin labelling, dynamic susceptibility contrast-enhanced perfusion-weighted imaging, and diffusion-weighted imaging. European Radiology, 2015, 25, 3423-3430.	4.5	49
130	Characterizing Resting-State Brain Function Using Arterial Spin Labeling. Brain Connectivity, 2015, 5, 527-542.	1.7	75
131	Simultaneous multi-slice Turbo-FLASH imaging with CAIPIRINHA for whole brain distortion-free pseudo-continuous arterial spin labeling at 3 and 7 T. NeuroImage, 2015, 113, 279-288.	4.2	57
132	Multi-vendor reliability of arterial spin labeling perfusion MRI using a near-identical sequence: Implications for multi-center studies. NeuroImage, 2015, 113, 143-152.	4.2	72
133	Associations of Resting-State fMRI Functional Connectivity with Flow-BOLD Coupling and Regional Vasculature. Brain Connectivity, 2015, 5, 137-146.	1.7	54
134	Decomposing cerebral blood flow MRI into functional and structural components: A non-local approach based on prediction. NeuroImage, 2015, 105, 156-170.	4.2	13
135	Impaired Cerebrovascular Function in Coronary Artery Disease Patients and Recovery Following Cardiac Rehabilitation. Frontiers in Aging Neuroscience, 2015, 7, 224.	3.4	41
136	Interhemispheric Cerebral Blood Flow Balance during Recovery of Motor Hand Function after Ischemic Stroke—A Longitudinal MRI Study Using Arterial Spin Labeling Perfusion. PLoS ONE, 2014, 9, e106327.	2.5	26
137	Anterior cingulate GABA levels predict whole-brain cerebral blood flow. Neuroscience Letters, 2014, 561, 188-191.	2.1	4
138	Detecting resting-state brain activity by spontaneous cerebral blood volume fluctuations using whole brain vascular space occupancy imaging. NeuroImage, 2014, 84, 575-584.	4.2	18
139	Dynamic and static contributions of the cerebrovasculature to the resting-state BOLD signal. NeuroImage, 2014, 84, 672-680.	4.2	51
140	Multi-delay arterial spin labeling perfusion MRI in moyamoya disease–comparison with CT perfusion imaging. European Radiology, 2014, 24, 1135-1144.	4.5	93
141	Transcranial electrical stimulation modifies the neuronal response to psychosocial stress exposure. Human Brain Mapping, 2014, 35, 3750-3759.	3.6	53
142	Reliability of twoâ€dimensional and threeâ€dimensional pseudoâ€continuous arterial spin labeling perfusion MRI in elderly populations: Comparison with 15oâ€water positron emission tomography. Journal of Magnetic Resonance Imaging, 2014, 39, 931-939.	3.4	93
143	Fast Local Trust Region Technique for Diffusion Tensor Registration Using Exact Reorientation and Regularization. IEEE Transactions on Medical Imaging, 2014, 33, 1005-1022.	8.9	12
144	Simultaneous fMRI–PET of the opioidergic pain system in human brain. Neurolmage, 2014, 102, 275-282.	4.2	59

#	Article	IF	CITATIONS
145	Metric Optimization for Surface Analysis in the Laplace-Beltrami Embedding Space. IEEE Transactions on Medical Imaging, 2014, 33, 1447-1463.	8.9	35
146	Multiple time scale complexity analysis of resting state FMRI. Brain Imaging and Behavior, 2014, 8, 284-291.	2.1	60
147	Effect of high dose isoflurane on cerebral blood flow in macaque monkeys. Magnetic Resonance Imaging, 2014, 32, 956-960.	1.8	49
148	Noncontrast enhanced fourâ€dimensional dynamic MRA with golden angle radial acquisition and kâ€space weighted image contrast (KWIC) reconstruction. Magnetic Resonance in Medicine, 2014, 72, 1541-1551.	3.0	33
149	Timeâ€resolved noncontrast enhanced 4â€D dynamic magnetic resonance angiography using multibolus TrueFISPâ€based spin tagging with alternating radiofrequency (TrueSTAR). Magnetic Resonance in Medicine, 2014, 71, 551-560.	3.0	18
150	Single-Subject Structural Networks with Closed-Form Rotation Invariant Matching Improve Power in Developmental Studies of the Cortex. Lecture Notes in Computer Science, 2014, 17, 137-144.	1.3	1
151	Regional Correlation between Resting State FDG PET and pCASL Perfusion MRI. Journal of Cerebral Blood Flow and Metabolism, 2013, 33, 1909-1914.	4.3	48
152	Quantitative mouse renal perfusion using arterial spin labeling. NMR in Biomedicine, 2013, 26, 1225-1232.	2.8	30
153	Regional cerebral blood flow alterations in obstructive sleep apnea. Neuroscience Letters, 2013, 555, 159-164.	2.1	51
154	Cortical responses to amphetamine exposure studied by pCASL MRI and pharmacokinetic/pharmacodynamic dose modeling. NeuroImage, 2013, 68, 75-82.	4.2	13
155	Balanced steady state free precession for arterial spin labeling MRI: Initial experience for blood flow mapping in human brain, retina, and kidney. Magnetic Resonance Imaging, 2013, 31, 1044-1050.	1.8	31
156	Multi-delay multi-parametric arterial spin-labeled perfusion MRI in acute ischemic stroke — Comparison with dynamic susceptibility contrast enhanced perfusion imaging. NeuroImage: Clinical, 2013, 3, 1-7.	2.7	180
157	Quantification of Network Perfusion in ASL Cerebral Blood Flow Data with Seed Based and ICA Approaches. Brain Topography, 2013, 26, 569-580.	1.8	25
158	Complexity and synchronicity of resting state blood oxygenation level-dependent (BOLD) functional MRI in normal aging and cognitive decline. Journal of Magnetic Resonance Imaging, 2013, 38, 36-45.	3.4	66
159	Periprocedural Arterial Spin Labeling and Dynamic Susceptibility Contrast Perfusion in Detection of Cerebral Blood Flow in Patients With Acute Ischemic Syndrome. Stroke, 2013, 44, 664-670.	2.0	20
160	Quantitative characterization of nuclear overhauser enhancement and amide proton transfer effects in the human brain at 7 tesla. Magnetic Resonance in Medicine, 2013, 70, 1070-1081.	3.0	85
161	Voxelwise Spectral Diffusional Connectivity and Its Applications to Alzheimer's Disease and Intelligence Prediction. Lecture Notes in Computer Science, 2013, 16, 655-662.	1.3	17
162	Turbo-FLASH Based Arterial Spin Labeled Perfusion MRI at 7 T. PLoS ONE, 2013, 8, e66612.	2.5	43

#	Article	IF	CITATIONS
163	Measurement of Cerebral White Matter Perfusion Using Pseudocontinuous Arterial Spin Labeling 3T Magnetic Resonance Imaging – an Experimental and Theoretical Investigation of Feasibility. PLoS ONE, 2013, 8, e82679.	2.5	38
164	The Value of Arterial Spin-Labeled Perfusion Imaging in Acute Ischemic Stroke. Stroke, 2012, 43, 1018-1024.	2.0	151
165	Longitudinal Reproducibility and Accuracy of Pseudo-Continuous Arterial Spin–labeled Perfusion MR Imaging in Typically Developing Children. Radiology, 2012, 263, 527-536.	7.3	86
166	Noncontrast dynamic MRA in intracranial arteriovenous malformation (AVM): comparison with time of flight (TOF) and digital subtraction angiography (DSA). Magnetic Resonance Imaging, 2012, 30, 869-877.	1.8	59
167	Applications of arterial spin labeled MRI in the brain. Journal of Magnetic Resonance Imaging, 2012, 35, 1026-1037.	3.4	272
168	Comparison of pulsed and pseudocontinuous arterial spinâ€labeling for measuring CO ₂ â€induced cerebrovascular reactivity. Journal of Magnetic Resonance Imaging, 2012, 36, 312-321.	3.4	30
169	A twoâ€stage approach for measuring vascular water exchange and arterial transit time by diffusionâ€weighted perfusion MRI. Magnetic Resonance in Medicine, 2012, 67, 1275-1284.	3.0	66
170	Quantification of arterial cerebral blood volume using multiphaseâ€balanced SSFPâ€based ASL. Magnetic Resonance in Medicine, 2012, 68, 130-139.	3.0	24
171	Comparison of arterial transit times estimated using arterial spin labeling. Magnetic Resonance Materials in Physics, Biology, and Medicine, 2012, 25, 135-144.	2.0	33
172	Fast Diffusion Tensor Registration with Exact Reorientation and Regularization. Lecture Notes in Computer Science, 2012, 15, 138-145.	1.3	2
173	Loss of Coherence of Low Frequency Fluctuations of BOLD FMRI in Visual Cortex of Healthy Aged Subjects. Open Neuroimaging Journal, 2011, 5, 105-111.	0.2	36
174	Baseline <i>CBF</i> , and <i>BOLD, CBF</i> , and <i>CMRO</i> ₂ fMRI of Visual and Vibrotactile Stimulations in Baboons. Journal of Cerebral Blood Flow and Metabolism, 2011, 31, 715-724.	4.3	41
175	Cerebral blood flow changes associated with different meditation practices and perceived depth of meditation. Psychiatry Research - Neuroimaging, 2011, 191, 60-67.	1.8	96
176	Serotonin transporter genotype modulates the association between depressive symptoms and amygdala activity among psychiatrically healthy adults. Psychiatry Research - Neuroimaging, 2011, 193, 161-167.	1.8	17
177	Test–retest reliability of arterial spin labeling with common labeling strategies. Journal of Magnetic Resonance Imaging, 2011, 33, 940-949.	3.4	214
178	Potentials and Challenges for Arterial Spin Labeling in Pharmacological Magnetic Resonance Imaging. Journal of Pharmacology and Experimental Therapeutics, 2011, 337, 359-366.	2.5	91
179	Quantification of Load Dependent Brain Activity in Parametric N-Back Working Memory Tasks using Pseudo-continuous Arterial Spin Labeling (pCASL) Perfusion Imaging. Journal of Cognitive Science, 2011, 12, 129-149.	0.2	4
180	Relationships between Cerebral Blood Flow and IQ in Typically Developing Children and Adolescents. Journal of Cognitive Science, 2011, 12, 151-170.	0.2	19

#	Article	IF	CITATIONS
181	In vivo venous blood <i>T</i> ₁ measurement using inversion recovery trueâ€FISP in children and adults. Magnetic Resonance in Medicine, 2010, 64, 1140-1147.	3.0	69
182	Estimation of perfusion and arterial transit time in myocardium using freeâ€breathing myocardial arterial spin labeling with navigatorâ€echo. Magnetic Resonance in Medicine, 2010, 64, 1289-1295.	3.0	41
183	Quantification Issues in Arterial Spin Labeling Perfusion Magnetic Resonance Imaging. Topics in Magnetic Resonance Imaging, 2010, 21, 65-73.	1.2	63
184	Unenhanced Dynamic MR Angiography: High Spatial and Temporal Resolution by Using True FISP–based Spin Tagging with Alternating Radiofrequency. Radiology, 2010, 256, 270-279.	7.3	67
185	Multiâ€echo balanced <scp>SSFP</scp> with a sequential phaseâ€encoding order for functional <scp>MR</scp> imaging at <scp>7T</scp> . Magnetic Resonance in Medicine, 0, , .	3.0	2